Dynamic modeling of non-cylindrical curved viscoelastic single-walled carbon nanotubes based on the second gradient theory

Materials Research Express

PAPER

Dynamic modeling of non-cylindrical curved viscoelastic single-walled carbon nanotubes based on the second gradient theory

RECEIVED
24 January 2019

REVISED
2 April 2019

ACCEPTED FOR PUBLICATION
4 April 2019

PUBLISHED
17 April 2019

Mohammad Malikan[1,4], **Van Bac Nguyen**[2], **Rossana Dimitri**[3] **and Francesco Tornabene**[3]

[1] Department of Mechanical Engineering, Faculty of Engineering, Islamic Azad University, Mashhad Branch, Mashhad, Iran
[2] College of Engineering and Technology, Department of Mechanical Engineering and the Built Environment, University of Derby, Derbyshire, United Kingdom
[3] Department of Innovation Engineering, Università del Salento, Lecce, Italy
[4] Author to whom any correspondence should be addressed.

E-mail: mohammad.malikan@yahoo.com, vb.nguyen@derby.ac.uk, rossana.dimitri@unisalento.it and francesco.tornabene@unisalento.it

Keywords: non-cylindrical curved SWCNTs, Kelvin-Voigt viscoelastic, nonlocal strain gradient theory, galerkin approach

Abstract

This paper is devoted to the theoretical study of the dynamic response of non-cylindrical curved viscoelastic single-walled carbon nanotubes (SWCNTs). The curved nanotubes are largely used in many engineering applications, but it is challenging in understanding mechanically the dynamic response of these curved SWCNTs when considering the influences of the material viscosity. The viscoelastic damping effect on the dynamic response is considered here by using the Kelvin-Voigt viscoelastic model. A modified shear deformation beam theory is here employed to formulate the governing partial differential equations. When the SWCNTs are considered in a small scale model, quantum impacts are important for a correct evaluation of the mechanical response of the nanosystem. This is here investigated by embedding the well-known nonlocal strain gradient approach into the governing equations. The extracted equations are solved by utilizing the Galerkin analytical approach in which the governing partial differential equations are reduced to ordinary differential equations and numerical findings are achieved for various boundary conditions. In order to evaluate the efficiency of the proposed theory, the outcomes in terms of natural frequencies of the vibrating nanotubes are verified with respect to the available literature. It follows a vast systematic study, where several parameters are varied to investigate the influences of geometrical properties involving different polygons of the SWCNTs on the dynamic response.

1. Introduction

If it is assumed that the methods of nanotechnology's production have reached their golden age, then carbon nanotubes (CNTs) should be considered as golden kids of this era. Unique properties including mechanical, electrical, chemical, and magnetic ones of these carbon nanomaterials have allowed the generation of many functional applications in engineering. CNTs are typically referred to as single-walled and multi-walled carbon nanotubes.

Single-walled carbon nanotubes (SWCNTs) are defined as one dimensional cylindrically shaped allotropes of carbon that have a high surface area and aspect ratio (length-to-diameter ratio). They are made from one atom thick carbon nanosheets that form a hollow cylindrical shape during the chemical vapour deposition synthesis, as discussed by Iijima [1]. Its unique properties, including the high elasticity modulus and good tensile strength together with the extraordinary properties of the carbon nature of the nanotubes (because carbon is a low-weight material, very stable and simple to perform processes that are cheaper than metals to produce) have led to a meaningful research on the performance of CNTs over the last decades. A lot of theoretical and practical works have focused on the atomic and continuum structures of CNTs. Extensive efforts have also been made to test and characterize the mechanical properties such as the Young's modulus, the tensile strength and imperfect

mechanism, and also the effects of nanotubes' deformations on the electrical properties. This particular interest in nanotubes can be attributed to their unique structure and features [2].

Nanotubes are assumed to be cylindrical structures and their carbon atoms have the ability to covalently bond to other atoms or molecules creating a new molecule with customized properties. These nanostructures are being well studied under static and dynamic forces by engineers and researchers around the world because of the importance of identifying their mechanical properties and responses for the mechanical design of CNTs in nanotechnology. In reality, a SWCNT is a long and bent nanostructure and it does not have perfectly straight shape. Although there have been many studies about mechanical and dynamic responses of straight nanotubes, there have been very limited investigations about curved nanotubes. Mehdipour *et al* [3] studied a curved single-walled carbon nanotube in a vibrational position and placed it on an elastic medium. They employed the Euler–Bernoulli beam theory in conjunction with the Hamilton principle. The He's energy balance method was adopted to seek numerical results in which the amplitude frequency response of the curved SWCNTs embedded in a Pasternak elastic foundation was obtained. Cigeroglu and Samandari [4] examined the nonlinear natural frequencies of a curved double-walled carbon nanotube (DWCNT) system bridged on a polymer foundation on the basis of the differential quadrature numerical technique in order to discretize the partial differential equations of motion in a spatial domain, namely in a nonlinear set of algebraic equations of motion. They also studied the nonlinear van der Waals forces between inner and outer tubes. A classical beam theory was implemented in the energy formulation to derive the basic relations, whose results showed that it is possible to detect different vibration modes occurring at a single vibration frequency when CNTs vibrate in the out-of-phase vibration mode. For the first time, the chaotic behavior of a SWCNT with an initial curvature in shape (waviness along its axis) exposed to harmonic excitation frequencies was investigated by Mayoof and Hawwa [5]. The equations were formulated according to the elastic continuum mechanics theory, while assuming an Euler–Bernoulli displacement field. Soltani *et al* [6] discussed about the natural frequencies of a curved SWCNT subjected to an electric field on the base of an analytical solution procedure. The Euler–Bernoulli elastic beam approach was used to formulate the equilibrium equations on the nonlinear vibration. The beam also was embedded in a Winkler matrix and, the gained relations were computed numerically using the Galerkin approach. Arefi and Zenkour [7] evaluated the influence of an electromagnetic surround on the static bending of a laminated curved nonlocal beam. A sinusoidal shear deformation beam theory was also used to the obtain governing equations and nonlocal electro-magneto-elasticity relationships were employed to derive the governing equations of bending based on the principle of virtual work. Mohamed *et al* [8] presented a differential-integral quadrature numerical method to study free and forced vibrations of a local beam with initial deflection bridged on a nonlinear polymer medium. They compared the outcomes of the proposed solution method with the analytical results and for validation purposes, with a good agreement among them. Liu *et al* [9] carried out the wave propagation analysis in a SWCNT taking into account viscoelastic effects according to the nonlocal strain gradient theory combined with the Timoshenko beam approach. Tadi Beni *et al* [10] investigated the wave propagation in a thin nano shell bridged on a viscoelastic foundation accounting for the internal damping influence in the shell. The nano size effects were considered using the nonlocal strain gradient model. Zhen and Zhou [11] studied the wave propagation in a SWCNT subjected to an axial magnetic field in a thermal surround based on the nonlocal strain gradient theory. They also considered the internal damping and surface effects to the wave analysis. Tadi Beni *et al* [12] analyzed the wave dispersion for a DWCNT conveying fluid based on the nonlocal strain gradient model. They investigated the slip boundaries and examined the van der Waals interaction between tubes embedded in a Winkler matrix. The first-order shear deformation shell theory was employed to derive the governing equations for the wave dispersion. Ghadiri *et al* [13] showed the small scale effects for a SWCNT conveying viscous fluid under a critical flow velocity based on the cylindrical shell model and the nonlocal strain gradient theory. The results were calculated using the differential quadrature technique for different boundary conditions. Zeighampour and Tadi Beni [14] studied the natural frequencies of a fluid conveying DWCNT based on a couple stress theory. The relationships were based on the Donnell's shell theory and solved by the differential quadrature method for simple and clamped boundary conditions in which the nanotubes were lied in a visco-Pasternak surrounding. Mohammadi *et al* [15] developed the nonlocal strain gradient shell model for mechanical vibrations of a SWCNT conveying viscous fluid. They performed some molecular dynamics simulations to study the effects of the fluid flow on the vibrational behavior of the SWCNT. Zhen [16] modeled a fluid-conveying SWCNT based on nonlocal and surface impacts in order to analyze the wave propagation of nanotubes. The Kelvin-Voigt viscoelastic model was also used in the governing equations in order to consider structural damping effects.

The molecular dynamics simulation method is well known to be an accurate but costly approach from a computational standpoint. For this reason it has been scarcely used [15,17–20] to investigate CNTs under static and dynamic vibration conditions. However, as far as the nonlocal theories are concerned for the analysis of CNTs in several conditions, many research studies have been published in recent years [21–40] on the topic.

Based on the above-mentioned review, several theories and techniques have been developed and applied for studying the dynamic response of the nanotubes in various conditions. It is largely noticed that viscosity of nanomaterials can affect their mechanical strength and electrical properties. For example, advantages in mechanical strength, thermal and electrical conductivity make CNTs ideal for additives in polymer composites. However, the dispersion of the nanoscale phase within the polymer matrix and the initiation of large changes in viscosity can ultimately contribute to the formation of defects which do not facilitate the expected strengthening in the mechanical or electrical properties which should be achieved [41].

Using current engineering processes, the curved nanotubes are widely made and synthesized. However, it is challenging in understanding mechanically the dynamic characteristics and responses of CNTs in curved shapes. Although the increased attention on curved nanotubes, there has not been any investigation on their dynamic response considering the effect of the material viscosity. In addition, a complete knowledge about the mechanical response of non-cylindrical nanotubes is still lacking. It is no doubt that understanding the mechanical response of non-cylindrical CNTs can lead to some useful outcomes for the synthesize process, and the development of new nanotubes in many engineering applications. Therefore, the study in this paper focuses on the dynamic response of curved SWCNTs considering the influence of viscoelastic properties. In particular, a refined beam theory is employed to determine the governing equation of the problem. To take into account the small scale influence of the nanostructure, a nonlocal strain gradient theory is embedded into the governing equation. The developed theory considers both nonlocality and size-dependent properties. The Galerkin approach is adopted in order to convert the partial differential equation into an ordinary one with a simple process, while satisfying completely different boundary conditions. Hence, the results in various conditions are got; the natural frequencies of a nanotube are compared with those obtained from some available references from the literature and several parameters are examined to show the influence of viscoelasticity and geometrical properties including various cross sections of the nanotube on the dynamic response.

2. Theoretical modelling

2.1. Energy formulation

The structure and shape of a SWCNT are shown in figure 1 along with the selected Cartesian coordinate. The cylindrical and non-cylindrical shape of a cross section of the SWCNT is shown in figure 1(a) and the curved form (curvature) of the nanotube is depicted in figure 1(b).

It is already well known that a CNT is a rolled form of graphene sheets in which atoms of pure carbon are arranged in a plan two-dimensional (2D) surface. Atoms are connected to the neighbors' ones by covalent bonds (figure 2) which are chemical connections. Assuming full cylindricality for a nanotube might not be completely true and the nanotubes can be assumed as polygon beams. Thus, showing and analyzing a SWCNT in a polygon shape is interestingly addressed in this study.

According to a one-variable refined beam theory (OVFSDT), as presented in Ref. [27], the displacement field is described as

$$\begin{Bmatrix} u_1(x,\,z,\,t) \\ u_3(x,\,z,\,t) \end{Bmatrix} = \begin{Bmatrix} u_0(x,\,t) - z\dfrac{\partial w_0(x,\,t)}{\partial x} \\ w_0(x,\,t) + B\dfrac{\partial^2 w_0(x,\,t)}{\partial x^2} \end{Bmatrix} \tag{1}$$

in which $u_1(x, z, t)$, $u_3(x, z, t)$ represent the displacement components of points along the x and z-axis and $u_0(x, t)$ and $w_0(x, t)$ are the corresponding components at the mid-surface of the undeformed SWCNT along x and z-axis. Moreover, the z-coordinate denotes the thickness direction. B is an additional coefficient defined by

$$B = \frac{EI_c}{AG} \tag{2}$$

in which G and E denote the shear and Young's moduli, A is the cross section area of the nanotube, and I_c $\left(I_c = \int_A z^2 dA\right)$ stands for the moment of area of the cross section.

The curvature of the nanotube can be defined by the equation below [3]

$$\varphi(x) = e\,\sin\left(\frac{\pi x}{L}\right) \tag{3}$$

where e is a constant related to the curvature and L refers to the length of the curved SWCNT (according to figure 1).

Based on the Hamilton principle, the dynamic equilibrium of a domain can only be obtained by the variational method and the equation below leads to the governing equations of the problem, as follows

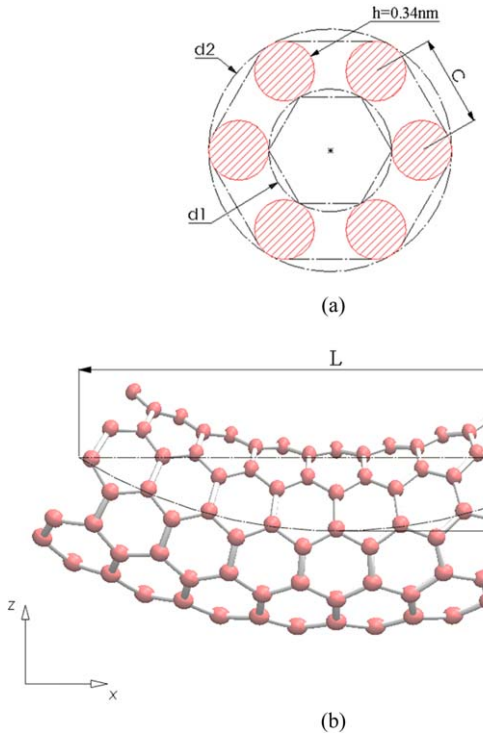

Figure 1. Cross section (a) and Curvature (b) of the nanotube (L displays the length, e shows values of the curvature, c is the length of the covalent bonds, h represents the thickness and the internal and external diameters are exhibited by d_1 and d_2, respectively for the SWCNT).

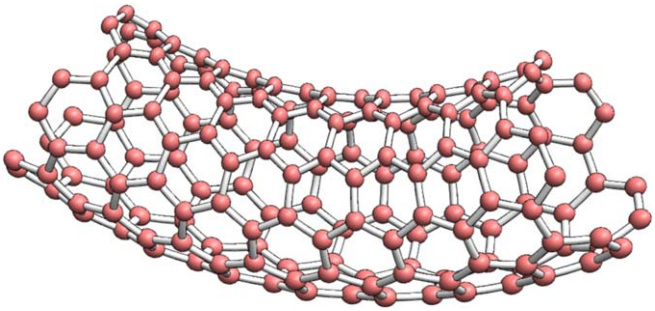

Figure 2. Three-dimensional scheme of the curved SWCNT.

$$\delta\Omega = \int_0^t (\delta U + \delta W - \delta K)dt = 0 \tag{4}$$

in which Ω refers to the nanotube's total potential energy, K and W stand for the kinetic energy and the work applied by exterior objects, U is symbolized for the strain energy of the system. Note that δ means the variations of the energies and time. In this study, the external forces applied on the nanotubes are not considered.

First of all, the strain energy in the variational form reads

$$\delta U = \frac{1}{2}\int\int_v\int \sigma_{xx}\delta\varepsilon_{xx} + \tau_{xz}\delta\gamma_{xz}dV = 0 \tag{5}$$

where δU is the virtual strain energy, σ_{xx}, τ_{xz}, ε_{xx} and γ_{xz} are the normal stress, shear stress, strains tensors at each point of the domain V. The tensor of nonlinear strains are obtained based on equation (1) as

$$\begin{Bmatrix} \varepsilon_{xx} \\ \gamma_{xz} \end{Bmatrix} = \begin{Bmatrix} \dfrac{\partial u_0}{\partial x} - z\dfrac{\partial^2 w_0}{\partial x^2} + \dfrac{\partial \varphi}{\partial x}\dfrac{\partial^2 w_0}{\partial x^2} + \dfrac{1}{2}\left(B\dfrac{\partial^3 w_0}{\partial x^3} + \dfrac{\partial w_0}{\partial x}\right)^2 \\ B\dfrac{\partial^3 w_0}{\partial x^3} \end{Bmatrix} \tag{6}$$

The Hookean elastic stress-strain relation is expressed as

$$\begin{Bmatrix} \sigma_{xx} \\ \tau_{xz} \end{Bmatrix} = [C_{ijkl}] \begin{Bmatrix} \varepsilon_{xx} \\ \gamma_{xz} \end{Bmatrix} \tag{7}$$

where C_{ijkl} is the stiffness matrix of the elasticity relation. Thereafter the strain energy of OVFSDT can be written as

$$\delta U = \int\int_v \int \left[\sigma_{xx} \left(\frac{\partial}{\partial x}\delta u_0 - z\frac{\partial^2}{\partial x^2}\delta w_0 + \frac{\partial \varphi}{\partial x}\frac{\partial^2}{\partial x^2}\delta w_0 + \left(B\frac{\partial^3}{\partial x^3}\delta w_0 + \frac{\partial}{\partial x}\delta w_0 \right)\left(B\frac{\partial^3 w_0}{\partial x^3} + \frac{\partial w_0}{\partial x} \right) \right) + B\tau_{xz}\frac{\partial^3}{\partial x^3}\delta w_0 \right] dV \tag{8}$$

The kinetic energy is given as

$$K = \frac{1}{2}\rho \int\int_A \left(\left(\frac{\partial u_1}{\partial t} \right)^2 + \left(\frac{\partial u_3}{\partial t} \right)^2 \right) dA dx = 0 \tag{9}$$

and the variational form of the kinetic energy is expressed as

$$\delta K = \rho \int\int_A \left[\left(-\frac{\partial^2 u_0}{\partial t^2} + z\frac{\partial^3 w_0}{\partial x \partial t^2} \right)\delta u_0 + \left(z\frac{\partial^3 u_0}{\partial x \partial t^2} - z^2\left(\frac{\partial^2 w_0}{\partial x \partial t} \right)^2 - z^2\frac{\partial^4 w_0}{\partial x^2 \partial t^2} - \frac{\partial^2 w_0}{\partial t^2} \right) - B^2\frac{\partial^6 w_0}{\partial x^4 \partial t^2} - 2B\frac{\partial^4 w_0}{\partial x^2 \partial t^2} \right)\delta w_0 \Bigg] dA dx = 0 \tag{10}$$

in which ρ is the sectional density, $m_0 \left(m_0 = \rho \int_A dA \right)$ shows the volumetric mass density and I_m ($I_m = \rho I_c$) is the mass moment of inertia.

By assigning $\delta\Omega = 0$, the constitutive equation can be expressed as

$$\delta u_0 : \frac{\partial N_x}{\partial x} - m_0\frac{\partial^2 u_0}{\partial t^2} = 0 \tag{11}$$

$$\delta w_0 : -\frac{\partial^2 M_x}{\partial x^2} + B\frac{\partial^3 Q_x}{\partial x^3} + N_x\left(B^2\frac{\partial^6 w_0}{\partial x^6} + 2B\frac{\partial^4 w_0}{\partial x^4} + \frac{\partial^2 w_0}{\partial x^2} + \frac{\partial^2 \varphi}{\partial x^2} \right) - I_m\left(\frac{\partial^4 w_0}{\partial x^2 \partial t^2} \right) - m_0\left(\frac{\partial^2 w_0}{\partial t^2} + B^2\frac{\partial^6 w_0}{\partial x^4 \partial t^2} + 2B\frac{\partial^4 w_0}{\partial x^2 \partial t^2} \right) = 0 \tag{12}$$

N_x, M_x and Q_x being the axial in-plane, moment and shear stress resultants, respectively.

Based on equation (7) the stress resultants are written as

$$\begin{Bmatrix} M_x \\ Q_x \\ N_x \end{Bmatrix} = \int_A \begin{Bmatrix} \sigma_x z \\ \tau_{xz} \\ \sigma_x \end{Bmatrix} dA \tag{13}$$

Therefore, equation (13) by means of equation (7) can be expanded as

$$\begin{Bmatrix} \mathrm{M_x} \\ \mathrm{Q_x} \\ \mathrm{N_x} \end{Bmatrix} = \begin{Bmatrix} -E(t)I_c\dfrac{\partial^2 w_0}{\partial x^2} \\ AG(t)\left(B\dfrac{\partial^3 w_0}{\partial x^3} \right) \\ E(t)A\left[\dfrac{\partial u_0}{\partial x} + \dfrac{\partial \varphi}{\partial x}\dfrac{\partial^2 w_0}{\partial x^2} + \dfrac{1}{2}\left(B\dfrac{\partial^3 w_0}{\partial x^3} + \dfrac{\partial w_0}{\partial x} \right)^2 \right] \end{Bmatrix} \tag{14}$$

In the following section, in order to investigate the effect of axial in-plane forces for the curved beam, the axial stress resultant in equation (14) leads to

$$N_x = E(t)A\left[\frac{\partial u_0}{\partial x} + \frac{\partial \varphi}{\partial x}\frac{\partial^2 w_0}{\partial x^2} + \frac{1}{2}\left(B\frac{\partial^3 w_0}{\partial x^3} + \frac{\partial w_0}{\partial x}\right)^2\right] = C_1 = Cte. \tag{15}$$

To determine the unknown quantity u_0 and calculate the constant C_1 in the previous equation, equation (15) can be integrated to have

$$u_0 = \int_0^L \left[-\frac{\partial \varphi}{\partial x}\frac{\partial^2 w_0}{\partial x^2} - \frac{1}{2}\left(B\frac{\partial^3 w_0}{\partial x^3} + \frac{\partial w_0}{\partial x}\right)^2\right]dx + \frac{C_1}{E(t)A}x + C_2 \tag{16}$$

where C_2 is an integration constant to be determined. By enforcing $u_0(0) = u_0(L) = 0$ on the equation (16), we get

$$\begin{cases} u_0|_{x=0} = \int_0^x \left[-\frac{\partial \varphi}{\partial x}\frac{\partial^2 w_0}{\partial x^2} - \frac{1}{2}\left(B\frac{\partial^3 w_0}{\partial x^3} + \frac{\partial w_0}{\partial x}\right)^2\right]dx\Big|_{x=0} + \frac{C_1}{E(t)A} \times 0 + C_2 \\ u_0|_{x=L} = \int_0^x \left[-\frac{\partial \varphi}{\partial x}\frac{\partial^2 w_0}{\partial x^2} - \frac{1}{2}\left(B\frac{\partial^3 w_0}{\partial x^3} + \frac{\partial w_0}{\partial x}\right)^2\right]dx\Big|_{x=L} + \frac{C_1}{E(t)A} \times L + C_2 \end{cases} \tag{17}$$

Upon mathematical rearrangement yields to

$$\Rightarrow \begin{cases} C_1 = \dfrac{E(t)A}{L} \times \displaystyle\int_0^L \left[\frac{\partial \varphi}{\partial x}\frac{\partial^2 w_0}{\partial x^2} + \frac{1}{2}\left(B\frac{\partial^3 w_0}{\partial x^3} + \frac{\partial w_0}{\partial x}\right)^2\right]dx \\ C_2 = 0 \end{cases} \tag{18}$$

2.2. Small scale effects

The small scale theories provide a constitutive framework on the continuum substance of nanomaterials and represent a good connection between the classic mechanics and nanomechanics. As a physical interpretation of Eringen's hypothesis (stress nonlocality) [42], in a continuum model, this theory incorporates long range force interactions between points of the domain. These interactions occur between charged atoms of a nanostructure. On the other hand, in the Mindlin strain gradient theory [43], the strain energy and elastic strains depend on their gradients. Therefore, in light of the gradients, this theory contains an additional coefficient with regard to the dimension of a length. Both these physical phenomena (nonlocal and strain gradient ones) can be combined to each other in a single theory called nonlocal strain gradient elasticity theory (NSGT) [44–53]. The NSGT includes the Eringen's nonlocal elasticity theory (Stress gradient) and the second gradient of strain of Mindlin (Strain gradient) [54] and can also account for the softening (decreasing stress at increasing strain) and hardening (increasing stress at decreasing strain) behavior of the material under deformation. Hence, the softening behavior can be considered as a result of stress nonlocality whereas the hardening behavior can be the result of a decreased size of the material. The small scale theories involving couple stress theories [55–59] or nonlocal elasticity theory of Eringen [60–64] have been extensively used in the previous studies. However, the efficiency and accuracy of the NSGT have been proved in comparison with the molecular mechanics [65, 66]. Therefore, the NSGT is adopted in this study via the following equation [67]

$$(1 - \mu\nabla^2)\sigma_{ij} = C_{ijkl}(1 - l^2\nabla^2)\varepsilon_{kl} \tag{19}$$

in which μ is the nonlocality ($\mu = (e_0 a)^2$); $\nabla^2 = \partial^2/\partial x^2 s$ and l represents a strain gradient length scale coefficient in the NSGT. These parameters should assume positive values according to the molecular mechanics and experimental works [68–72]. In this paper in order to have appropriate numerical outcomes, the amplitudes are used for both parameters. However, the most effective way to determine and measure the aforementioned intrinsic length scale parameters is the experimental testing or atomic modelling like molecular dynamics. It was found that the nonlocal parameter is in the range of $0 < e_0 a \leqslant 2$ nm [68] and a dimensionless parameter which should be a function of thickness of the structure, is used for the strain gradient length scale coefficient [71]. There have been other studies [69] where the value of the nonlocal parameter based on a molecular mechanics method showed that there might not have a unique value for such an intrinsic small scale parameter as the value is related to various conditions (e.g. the environmental influences, boundary conditions, atomic lattice and some internal conditions such as the crack situation in a cracked material). Hence, by assigning a reasonable value, as obtained from molecular mechanics for this nonlocal parameter, can be applicable for seeking numerical outcomes.

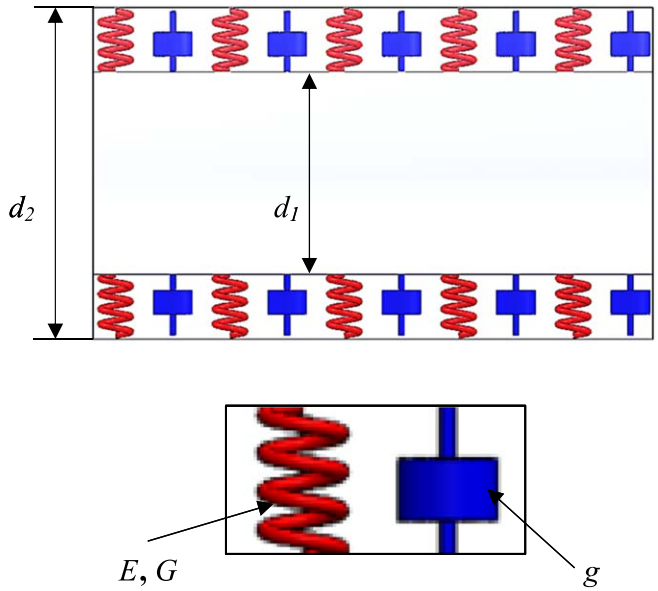

Figure 3. Schematic arrange of the Kelvin-Voigt model in a straight SWCNT.

Substituting equation (19) into equation (14), the small scale stress resultants read

$$(1 - \mu\nabla^2)M_x = -(1 - l^2\nabla^2)\left(E(t)I_c\frac{\partial^2 w_0}{\partial x^2}\right) \tag{20}$$

$$(1 - \mu\nabla^2)Q_x = (1 - l^2\nabla^2)AG(t)\left(B\frac{\partial^3 w_0}{\partial x^3}\right) \tag{21}$$

2.3. Viscoelasticity behavior

The material response in this research work is not limited to the elastic behavior. Most materials around us can undergo an internal damping when they are subjected to dynamic conditions. For a linear elastic material, the relationship for stress and strain is linearly proportional by means of the elastic modulus of the material, without considering the time variable. When we investigate the viscoelasticity, which is a time-dependent property for materials, the fluidity of the material's structures should be taken into account. For such materials the relationship between stress and strain can be expressed in several empirical models such that the simplest and non-trivial form can be the Kelvin-Voigt model [73]. This model is widely used in the theoretical research due to its simplicity [9–11, 46, 49, 65, 66]. In a schematic diagram the Kelvin-Voigt viscoelastic coupling contains a spring showing elastic property and dashpot displaying viscous property in a parallel series (figure 3). The constant elastic moduli for the Kelvin-Voigt model are

$$\begin{cases} E(t) = E\left(1 + g\dfrac{\partial}{\partial t}\right) \\ G(t) = G\left(1 + g\dfrac{\partial}{\partial t}\right) \end{cases} \tag{22}$$

in which g depicts the viscosity coefficient.

2.4. Frequency equation

In this subsection, by combining equations (11)–(12), (18), (20)–(22), the governing equation is determined. The resulting relation can be used to compute the natural frequencies of the non-cylindrical curved viscoelastic SWCNT.

$$(1-l^2\nabla^2)\left[\left(1+g\frac{\partial}{\partial t}\right)\left(EI_c\frac{\partial^4 w_0}{\partial x^4}+AGB^2\frac{\partial^6 w_0}{\partial x^6}\right)\right]-(1-l^2\nabla^2)$$
$$\times\left(1+g\frac{\partial}{\partial t}\right)\times\left\langle\frac{EA}{L}\times\int_0^L\left[\frac{\partial\varphi}{\partial x}\frac{\partial^2 w_0}{\partial x^2}+\frac{1}{2}\left(B\frac{\partial^3 w_0}{\partial x^3}+\frac{\partial w_0}{\partial x}\right)^2\right]dx\right.$$
$$\left.\times\left(B^2\frac{\partial^6 w_0}{\partial x^6}+2B\frac{\partial^4 w_0}{\partial x^4}+\frac{\partial^2 w_0}{\partial x^2}+\frac{\partial^2\varphi}{\partial x^2}\right)\right\rangle+(1-\mu\nabla^2)$$
$$\times\left[-I_m\left(\frac{\partial^4 w_0}{\partial x^2\partial t^2}\right)-m_0\left(\frac{\partial^2 w_0}{\partial t^2}+B^2\frac{\partial^6 w_0}{\partial x^4\partial t^2}+2B\frac{\partial^4 w_0}{\partial x^2\partial t^2}\right)\right]=0 \tag{23}$$

3. Solving method

In this study, the Galerkin technique is applied to reduce the partial differential equation (PDE) to an ordinary differential equation (ODE) as [6]

$$w_0(x,\,t)=y(x)\lambda(t) \tag{24}$$

in which $y(x)$ is the fundamental mode shape and $\lambda(t)$ is a temporary function based on time. The mode shapes according to different boundary conditions are shown below [6], namely

Clamped-Clamped (CC):

$$y(x)=\cosh\left(\frac{3\pi}{2}\frac{x}{L}\right)-0.9825\sinh\left(\frac{3\pi}{2}\frac{x}{L}\right)-\cos\left(\frac{3\pi}{2}\frac{x}{L}\right)+0.9825\sin\left(\frac{3\pi}{2}\frac{x}{L}\right) \tag{25}$$

Simple-Simple (SS):

$$y(x)=\sin\left(\pi\frac{x}{L}\right) \tag{26}$$

Upon substitution of equation (24) into equations (23), (23) reduces to an ODE after which for computing each boundary condition equations (25)–(26) can be used. In order to extract natural frequencies, the following analytical equation is employed

$$\lambda(t)=\exp(i\omega_n t),\ i=\sqrt{-1} \tag{27}$$

where $\omega_n$corresponds to the natural frequencies of the nanotube.

Consequently, solving the equation below based on the ω_n and after some manipulation and simplification, the natural frequency of the SWCNT would be computed (dot (.) denotes derivatives).

$$\int_0^{L_x}[\eta\ddot{\lambda}(t)+\zeta\dot{\lambda}(t)+\lambda]y(x)dx=0 \tag{28}$$

where the coefficients η, ζ and λ are detailed in appendix A.

4. Verifying the present model

Prior to computing the natural frequencies in different conditions, the accuracy of the presented theory has been proved. Table 1 presents the results obtained by different well-known beam theories against the present theory. As can be observed, the findings of the present study are in good agreement with those taken by the previous studies [49, 74, 75]. In particular, an increased length-to-thickness ratio of the beam (which results in thinner beams), makes the results closer for various shear deformation beam theories as illustrated in table 1. On the other hand, for moderately thick and thick beams, shear deformations are more significant, therefore the results based on an Euler–Bernoulli theory become different than those ones from other theories, see, for example the results at $e_0a=0$, $L/h=5$. In particular, when L/h increases from 5 to 10 and 20, the natural frequencies taken by the Euler–Bernoulli theory and OVFSDTs' differ from the other ones of about 4%, 1.2% and 0.3%, respectively.

In addition, table 2 shows the results from [19, 27] based on a nonlocal elasticity theory, strain gradient theory and nonlocal strain gradient theory, compared with the results obtained from the present theory. In the table, the CNT was modeled using the first-order shear deformation theory. The natural frequencies were computed by using the Navier's solution technique [19, 27] and molecular dynamics simulation (MD) [19] for simply-supported boundary conditions. It can be clearly observed that the pure strain gradient theory ($\mu_0=0$, $l\neq 0$) was unable to give accurate results, especially for small length ratios L/D. Moreover, the greater the length

Table 1. A comparison for dimensionless natural frequencies of a nanobeam as provided by different theories.

					Timoshenko beam theory (TBT)		Sinusoidal beam theory (SBT)	
L/h	$(e_0a)^2$	OVFSDT, Galerkin [Present]	OVFSDT, Navier [49]	Euler–Bernoulli theory (EBT) [75]	[74]	[75]	[74]	[75]
5	0	9.2808	9.2943	9.7112	9.2740	9.2740	9.2752	9.2752
	1	8.8463	8.8587	9.2647	8.8477	8.8477	8.8488	8.8488
	2	8.4696	8.4788	8.8747	8.4752	8.4752	8.4763	8.4763
	3	8.1399	8.1495	8.5301	8.1461	8.1461	8.1472	8.1472
	4	7.8629	7.8693	8.2228	7.8526	7.8526	7.8536	7.8536
10	0	9.7121	9.7209	9.8293	9.7075	9.7075	9.7077	9.7077
	1	9.2580	9.2666	9.3774	9.2612	9.2612	9.2614	9.2614
	2	8.8773	8.8857	8.9826	8.8713	8.8713	8.8715	8.8715
	3	8.5401	8.5483	8.6338	8.5269	8.5269	8.5271	8.5271
	4	8.2241	8.2320	8.3228	8.2196	8.2196	8.2198	8.2198
20	0	9.8300	9.8377	9.8595	9.8281	9.8281	9.8282	9.8282
	1	9.3787	9.3840	9.4062	9.3763	9.3763	9.3764	9.3764
	2	8.9866	8.9917	9.0102	8.9816	8.9816	8.9816	8.9816
	3	8.6416	8.6456	8.6604	8.6328	8.6328	8.6329	8.6329
	4	8.3309	8.3329	8.3483	8.3218	8.3218	8.3218	8.3218

$\Omega_n = \omega_n L^2\sqrt{\frac{\rho A}{EI}}, E = 1$ TPa, $\upsilon = 0.3, h = 1$ nm, $m = 0.9$ to 1.1.

of the nanotube, the closer the results of the nonlocal strain gradient case ($\mu_0 \neq 0, l \neq 0$) in comparison with the MD outcomes.

5. Numerical analysis of frequency

In this section, we investigate and evaluate the length scale and the nonlocal parameter effects on the dimensionless natural frequency of the nanotube, while considering different cross sections, curvature influences, internal viscosity, and boundary conditions. The mechanical properties of the problem are selected in agreement with Refs. [17, 74–76].

Table 2. Validation of natural frequencies (THz) for a nanotube obtained by different small scale theories.

		Nonlocal strain gradient theory		Strain gradient theory		Nonlocal elasticity theory	
L/D	[19] (MD)	[19]	Present, [27]	[19]	Present, [27]	[19]	Present, [27]
4.86	1.138	1.209	1.25535	12.42	12.35233	0.758	0.75967
8.47	0.466	0.448	0.43207	4.461	4.69543	0.333	0.35485
13.89	0.190	0.192	0.19004	1.957	1.98552	0.165	0.16355
17.47	0.122	0.126	0.12431	1.321	1.22947	0.121	0.12460

$E = 1.06$ TPa, $\upsilon = 0.19, h = 0.34$ nm, $d = 0.68$ nm, SS.
$e_0a = 3.3$ to 3.5 nm, $l = 0.1$ to 0.4 nm.

$$E = 1\ \text{TPa},\ \nu = 0.3,\ h = 0.34\ \text{nm},\ \rho = 2300\ \text{kg m}^{-3},$$
$$d_2 = 1\ \text{nm},\ r_2 = d_2/2,\ r_1 = r_2 - h,$$
$$Cylindrical\ type\ (CT),\ Non-cylindrical\ type\ (NCT),$$
$$8P(Octagonal\ NCT) \rightarrow I_c = 0.6381(r_2^4 - r_1^4)$$
$$6P(Hexagonal\ NCT) \rightarrow I_c = 0.5409(r_2^4 - r_1^4)$$
$$Non-dimensional\ natural\ frequency\text{:}\ \Omega_n = \omega_n L^2\sqrt{\frac{\rho A}{EI_c}}$$

In figure 4(a), the variation of the length scale parameter versus the size e^* for the SWCNT on the natural frequencies was investigated. For this purpose, a simple-simple (SS) boundary condition was selected. As it can be seen, increasing the amount of curvature of the nanotube increases its rigidity, and consequently increases the amount of the non-dimensional natural frequencies. Interestingly, the increase in the natural frequency seems to be very sharp. On the other hand, increasing values of the length scale parameter increase the material stiffness. As a result, the natural frequency values become higher. Figure 4(b) also shows the variation of the curvature of the nanotube for different values of the nonlocal parameter. It is interesting to note that, increasing the nonlocal parameter, decreases the stiffness of the nanotube. From both figures it can be found that the increase in curvature resulted in the increase in the distances of diagrams' curves (results related to $l = 0$ to $l = h$ and $e_0a = 0$ to $e_0a = 2$ nm) leading the curvature to be important. Ultimately, for large quantities of e_0a, the nonlocal parameter decreases the stiffness of the SWCNT even with the increase of e^*.

Figure 5 examines the effect of the curvature on the natural frequencies for different boundary conditions. It is clear that the use of a clamped-clamped (CC) boundary condition leads to higher natural frequency values whereby a SS boundary condition leads to lower natural frequencies. It is also noted that the effect of the increase in the curvature on the CC boundary condition was more pronounced with lower effects on the SS boundary condition. Furthermore, an increasing length of the tube is more evident in clamped boundaries.

Figure 6 plots the effects of viscoelasticity on the curvature of the SWCNT. It can be seen that, by increasing the interior viscosity of the nanotube, the amount of stiffness increases together with an increased natural frequency. For increasing values of e^*, the effect of the curvature on the natural frequency was more pronounced for larger values of viscosity (the distances between frequency results obtained from different values of g in the region of lowest values of e^* ($\sim$0.05) are much smaller than those in the region of the largest values of e^* ($\sim$2)). Hence, for larger values of e^*, the variation of the non-dimensional natural frequency for different viscosities becomes even more significant for increasing curvatures. This confirms the effects of the material viscosity on the vibration response of the curved CNTs.

Figure 7(a) shows the effects of the non-cylindrical shape on the natural frequencies of CNTs. As can be seen, the SWCNT is assumed to be in three shapes: cylindrical, hexagonal, and octagonal shapes. According to the outcomes, the natural frequency values of a non-cylindrical nanotube is greater than those ones of a cylindrical nanotube and the nanotube features the lowest natural frequency values. It is also interesting to note that, when the curvature and bending of the nanotube become larger, the results of different sections differed from each other, and it is proved that in nanotubes with a large initial curvature it is important to consider the actual cross section of the nanotube.

Figure 7(b) illustrates the viscosity effect for the three shapes of the CNT mentioned above namely with cylindrical, hexagonal, and octagonal shapes. As shown in the previous figures, the increase in internal viscosity results in an increase in the natural frequency of the SWCNTs, which is reaffirmed in figure 7(b). On the other hand, the importance of the above results is that the increase of the parameter g results in the parallel curves for

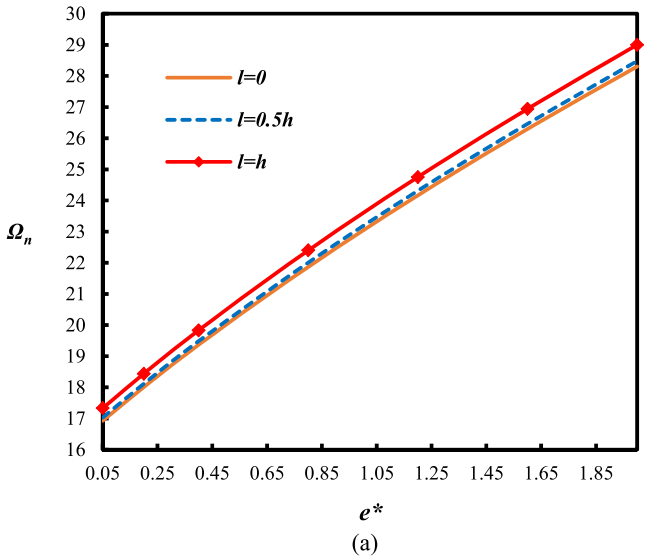

(a)

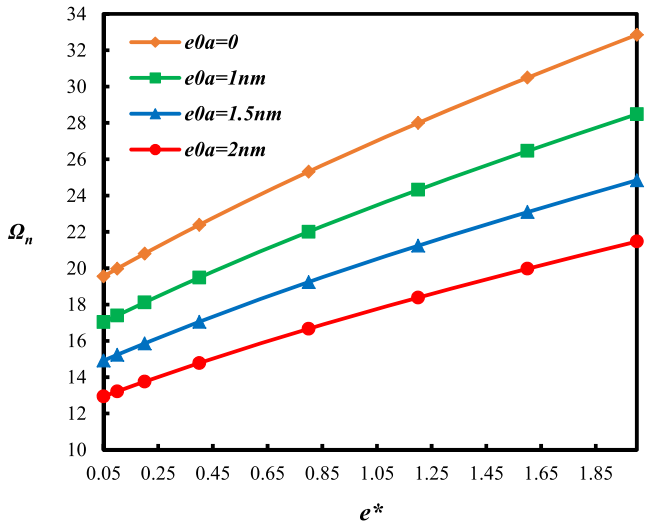

(b)

Figure 4. (a) Effect of the curvature versus several length scale parameters on the natural frequencies of the SWCNTs ($e_0a = 1$ nm, $e^* = e/d, g = 1N.s/m, L = 5d, SS, CT$).(b) Effect of the curvature versus several nonlocal parameters on the natural frequencies of the SWCNTs ($l = 0.5$ h, $e^* = e/d, g = 1N.s/m, L = 5d, SS, CT$).

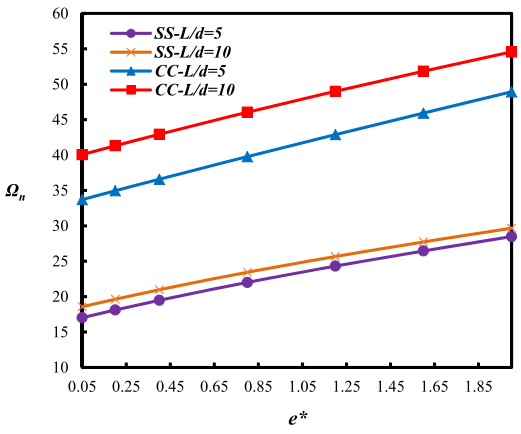

Figure 5. Effect of the curvature versus different boundary conditions on the natural frequencies of the SWCNTs ($e_0a = 1$ nm, $l = 0.5$ h, $e^* = e/d, g = 1$ $N.s/m, L = 5d, CT$).

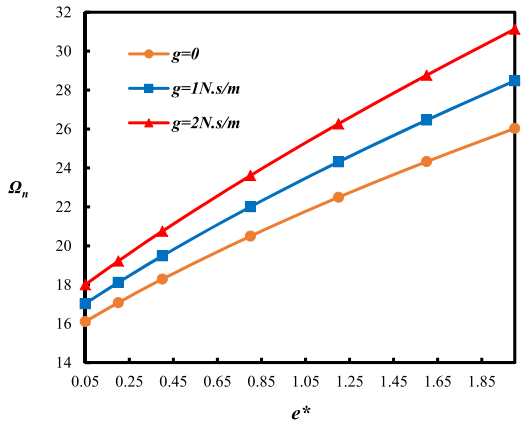

Figure 6. Effect of the curvature versus viscosity on the natural frequencies of the SWCNTs ($e_0a = 1$ nm, $l = 0.5$ h, $e^* = e/d$, $L = 5d$, *SS*, *CT*).

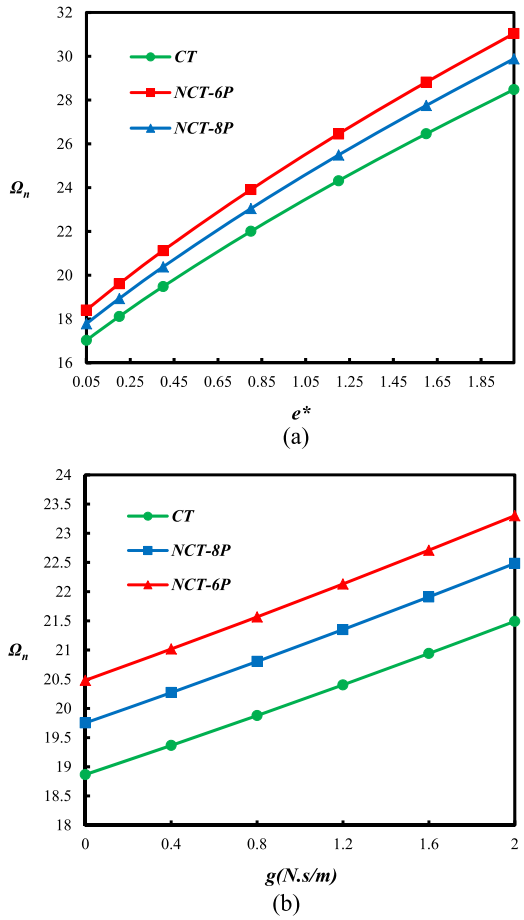

Figure 7. (a) Effect of the curvature versus several cross sections on the natural frequencies of the SWCNTs ($e_0a = 1$ nm, $l = 0.5$ h, $g = 1$ *N.s/m*, $e^* = e/d$, $L = 5d$, *SS*). (b) Effect of the viscosity versus several cross sections on the natural frequencies of the SWCNTs ($e_0a = 1$ nm, $l = 0.5$ h, $e = 0.5d$, $L = 5d$, *SS*).

the three sections. In conclusion, the increase of the curvature leads to an increased importance of the selected section of the nanotube.

Figures 8(a)–(c) demonstrate the nonlocal parameter effect for SS and CC boundary conditions, and the effect of changing the length scale parameter values for the SS boundary condition on the results for each shape.

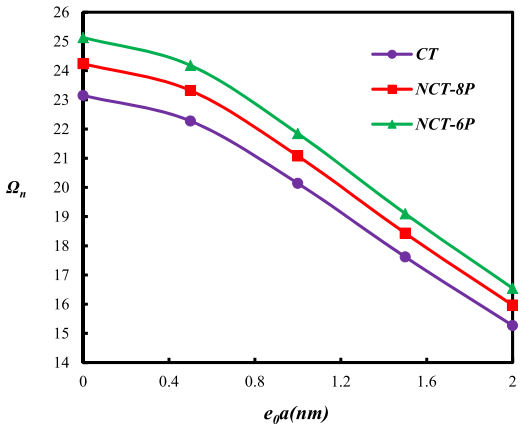

(a)

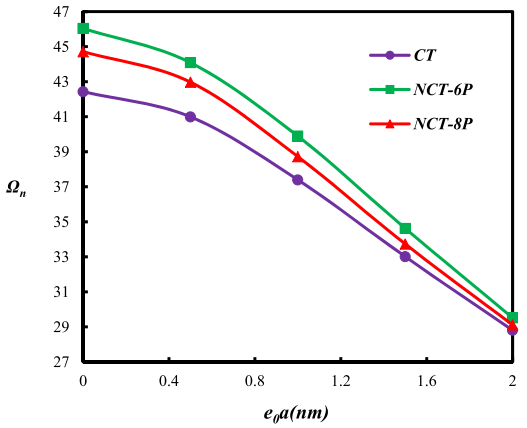

(b)

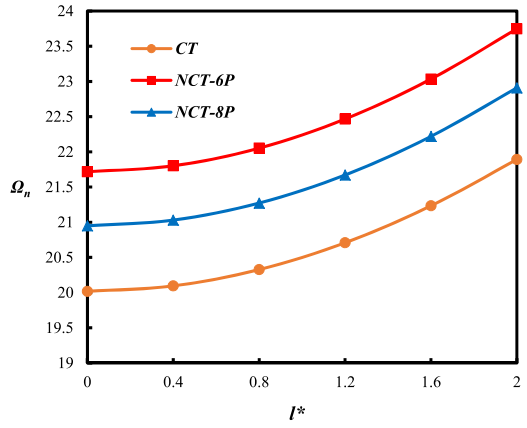

(c)

Figure 8. (a) Effect of the nonlocal parameter versus several cross sections on the natural frequencies of the SWCNTs ($l = 0.5$ h, $g = 1N.s/m$, $e = 0.5d$, $L = 5d$, *SS*). (b) Effect of the nonlocal parameter versus several cross sections on the natural frequencies of the SWCNTs ($l = 0.5$ h, $g = 1N.s/m$, $e = 0.5d$, $L = 5d$, *CC*). (c) Effect of the length scale parameter versus several cross sections on the natural frequencies of the SWCNTs ($e_0a = 1$ nm, $l^* = l/h$, $g = 1N.s/m$, $e = 0.5d$, $L = 5d$, *SS*).

From these figures, it can be seen that increasing the nonlocal parameter values gets to closer results for the NCT and CT cross sections. However, this result is more noticeable in the second figure and for CC boundary conditions. For large values of the nonlocal parameter, especially if the number of sides is large, it does not make much difference based on what the cross section of the nanotubes is. Indeed, the results of octagonal and cylinder sections do not differ for larger values of the nonlocal parameter. It is also demonstrated in figure 8(c) that the nanotube's cross section does not affect the length scale parameter. One might conclude that the nonlocal parameter has more geometric effects than the length scale parameter.

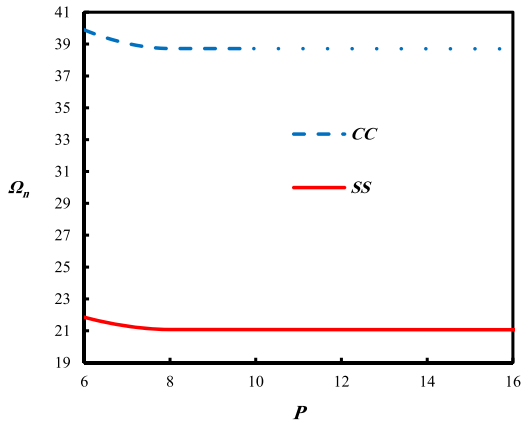

Figure 9. Effect of the number of the cross sections versus different boundary conditions on the natural frequencies of the SWCNTs ($e_0a = 1$ nm, $l = 0.5$ h, $g = 1N.s/m$, $e = 0.5d$, $L = 5d$).

Finally, figure 9 describes the boundary conditions for various cross section shapes. It is worth mentioning that from the hexagonal to the cylindrical (infinite number of sides) shapes, the results of the CC boundary condition lead to a more pronounced increase in the CC boundary condition than the SS one. Also, the difference between results according to different boundary conditions decreases by increasing the number of polygons.

6. Conclusions

Curved CNTs were studied with cylindrical and non-cylindrical cross section shapes, taking into account the influences of the material viscosity on the natural frequencies of the nanotube. The nonlocal strain gradient governing equation was obtained based on a modified beam approach. The finalized partial differential equation was converted into an ordinary differential equation using the Galerkin method in which some approximate mode shapes were obtained, satisfying various boundary conditions. Then, the numerical outcomes were gained and some important research points can be highlighted as follows:

- Increasing the curvature of the SWCNTs significantly increased the influence of material viscosity on the vibration response of SWCNTs.
- The curvature of the nanotube deemed to make the nanotubes stiffer, leading to higher natural frequencies in vibration.
- By increasing the curvature of the SWCNT, the natural frequencies for both the nonlocal and length scale parameter values became far from each other, leading to the significant influences of curvature of the CNTs in the small scale model.
- Whilst clamped-clamped boundary condition was taken into consideration, by increasing the nonlocal parameter, the natural frequency values of various cross section's shapes tended to be closer to each other. This confirmed that the nonlocality had further impacts in the cases of more rigid boundary conditions.
- The curvature of the nanotube affects the natural frequency for different cross sections.

Acknowledgments

The authors would like to thank the reviewers for their insightful comments on the paper, which improved significantly the work.

Appendix A

$$\eta = -[I_m\ddot{y}(x) + m_0(1 + B^2\ddot{y}(x) + 2B\ddot{y}(x))] + \mu[I_m\ddot{\ddot{y}}(x) + m_0(1 + B^2\ddot{\ddot{y}}(x) + 2B\ddot{y}(x))]$$

$$\zeta = [g(EI_c\ddot{y}(x) + AGB^2\ddot{\ddot{y}}(x))] - l^2[g(EI_c\ddot{\ddot{y}}(x) + AGB^2\ddot{\ddot{y}}(x))] - g$$

$$\times\left\langle \frac{EA}{L} \times \int_0^L \left[\dot{\varphi}(x)\dot{y}(x) + \frac{1}{2}(B\ddot{y}(x) + \dot{y}(x))^2\right]dx \times (B^2\ddot{\ddot{y}}(x) + 2B\ddot{y}(x) + \ddot{y}(x) + \ddot{\varphi}(x))\right\rangle + l^2g$$

$$\times\left\langle \frac{EA}{L} \times \int_0^L \left[\dot{\varphi}(x)\dot{y}(x) + \frac{1}{2}(B\ddot{y}(x) + \dot{y}(x))^2\right]dx \times (B^2\ddot{\ddot{y}}(x) + 2B\ddot{\ddot{y}}(x) + \ddot{y}(x) + \ddot{\varphi}(x))\right\rangle$$

$$\lambda = [(EI_c\ddot{y}(x) + AGB^2\ddot{\ddot{y}}(x))] - l^2[(EI_c\ddot{\ddot{y}}(x) + AGB^2\ddot{\ddot{y}}(x))]$$

$$-\left\langle \frac{EA}{L} \times \int_0^L \left[\dot{\varphi}(x)\dot{y}(x) + \frac{1}{2}(B\ddot{y}(x) + \dot{y}(x))^2\right]dx \times (B^2\ddot{\ddot{y}}(x) + 2B\ddot{y}(x) + \ddot{y}(x) + \ddot{\varphi}(x))\right\rangle$$

$$+ l^2\left\langle \frac{EA}{L} \times \int_0^L \left[\dot{\varphi}(x)\dot{y}(x) + \frac{1}{2}(B\ddot{y}(x) + \dot{y}(x))^2\right]dx \times (B^2\ddot{\ddot{y}}(x) + 2B\ddot{\ddot{y}}(x) + \ddot{y}(x) + \ddot{\varphi}(x))\right\rangle$$

ORCID iDs

Mohammad Malikan https://orcid.org/0000-0001-7356-2168

References

[1] Iijima S and Ichihashi T 1993 Single-shell carbon nanotubes of 1-nm diameter *Nature* **363** 603–35
[2] Iijima S 1991 Helical microtubes of graphitic carbon *Nature* **354** 56–8
[3] Mehdipour I, Barari A, Kimiaeifar A and Domairry G 2012 Vibrational analysis of curved single-walled carbon nanotube on a Pasternak elastic foundation *Adv. Eng. Softw.* **48** 1–5
[4] Cigeroglu E and Samandari H 2014 Nonlinear free vibrations of curved double walled carbon nanotubes using differential quadrature method *Physica* E **64** 95–105
[5] Mayoof F N and Hawwa M A 2009 Chaotic behavior of a curved carbon nanotube under harmonic excitation *Chaos Solitons Fractals* **42** 1860–7
[6] Soltani P, Kassaei A and Taherian M M 2014 Nonlinear and quasi-linear behavior of a curved carbon nanotube vibrating in an electric force field; analytical approach *Acta Mech. Solida Sin.* **27** 97–110
[7] Arefi M and Zenkour A 2017 Influence of magneto-electric environments on size-dependent bending results of three-layer piezomagnetic curved nanobeam based on sinusoidal shear deformation theory *Journal of Sandwich Structures & Materials* (https://doi.org/10.1177/1099636217723186)
[8] Mohamed N, Eltaher M A, Mohamed S A and Seddek L F 2018 Numerical analysis of nonlinear free and forced vibrations of buckled curved beams resting on nonlinear elastic foundations *Int. J. Non-Linear Mech.* **101** 157–73
[9] Yugang T, Liu Y and Zhao D 2017 Wave dispersion in viscoelastic single walled carbon nanotubes based on the nonlocal strain gradient Timoshenko beam model *Physica E: Low-dimensional Systems and Nanostructures* **87** 301–7
[10] Zeighampour H, Tadi Beni Y and Botshekanan Dehkordi M 2018 Wave propagation in viscoelastic thin cylindrical nanoshell resting on a visco-Pasternak foundation based on nonlocal strain gradient theory *Thin-Walled Struct.* **122** 378–86
[11] Zhen Y and Zhou L 2017 Wave propagation in fluid-conveying viscoelastic carbon nanotubes under longitudinal magnetic field with thermal and surface effect via nonlocal strain gradient theory *Modern Physics Letters* B **31** 1750069
[12] Zeighampour H, Tadi Beni Y and Karimipour I 2017 Wave propagation in double-walled carbon nanotube conveying fluid considering slip boundary condition and shell model based on nonlocal strain gradient theory *Microfluidics and Nanofluidics* **21** 85
[13] Mahinzare M, Mohammadi K, Ghadiri M and Rajab Pour A 2017 Size-dependent effects on critical flow velocity of a SWCNT conveying viscous fluid based on nonlocal strain gradient cylindrical shell model *Microfluidics and Nanofluidics* **21** 123
[14] Zeighampour H and Beni Y T 2014 Size-dependent vibration of fluid-conveying double-walled carbon nanotubes using couple stress shell theory *Physica E: Low-dimensional Systems and Nanostructures* **61** 28–39
[15] Mohammadi K, Rajabpour A and Ghadiri M 2018 Calibration of nonlocal strain gradient shell model for vibration analysis of a CNT conveying viscous fluid using molecular dynamics simulation *Comput. Mater. Sci.* **148** 104–15
[16] Zhen Y-X 2017 Wave propagation in fluid-conveying viscoelastic single-walled carbon nanotubes with surface and nonlocal effects *Physica E: Low-dimensional Systems and Nanostructures* **86** 275–9
[17] Hwang C C, Wang Y C, Kuo Q Y and Lu J M 2010 Molecular dynamics study of multi-walled carbon nanotubes under uniaxial loading *Physica* E **42** 775–8
[18] Ansari R, Ajori S and Arash B 2012 Vibrations of single- and double-walled carbon nanotubes with layerwise boundary conditions: a molecular dynamics study *Current Applied Physics* **12** 707–11
[19] Mehralian F, Tadi Beni Y and Karimi Zeverdejani M 2017 Nonlocal strain gradient theory calibration using molecular dynamics simulation based on small scale vibration of nanotubes *Physica B: Condensed Matter* **514** 61–9
[20] Mehralian F, Tadi Beni. Y and Karimi Zeverdejani M 2017 Calibration of nonlocal strain gradient shell model for buckling analysis of nanotubes using molecular dynamics simulations *Physica B: Condensed Matter* **521** 102–11
[21] Arghavan S and Singh A V 2011 On the vibrations of single-walled carbon nanotubes *J. Sound Vib.* **330** 3102–22
[22] Fang B, Zhen Y X, Zhang C P and Tang Y 2013 Nonlinear vibration analysis of double-walled carbon nanotubes based on nonlocal elasticity theory *Appl. Math. Modelling* **37** 1096–107

[23] Brischetto S 2014 A continuum elastic three-dimensional model for natural frequencies of single-walled carbon nanotubes *Composites Part B: Engineering* **61** 222–8
[24] Wang Y Z and Li F M 2014 Nonlinear free vibration of nanotube with small scale effects embedded in viscous matrix *Mech. Res. Commun.* **60** 45–51
[25] Rahmanian M, Torkaman-Asadi M A, Firouz-Abadi R D and Kouchakzadeh M A 2016 Free vibrations analysis of carbon nanotubes resting on Winkler foundations based on nonlocal models *Physica B: Condensed Matter* **484** 83–94
[26] Fernandes R, El-Borgi S, Mousavi S M, Reddy J N and Mechmoum A 2017 Nonlinear size-dependent longitudinal vibration of carbon nanotubes embedded in an elastic medium *Physica E: Low-Dimensional Systems and Nanostructures* **88** 18–25
[27] Malikan M, Nguyen V B and Tornabene F 2018 Damped forced vibration analysis of single-walled carbon nanotubes resting on viscoelastic foundation in thermal environment using nonlocal strain gradient theory *Engineering Science and Technology, an International Journal* **21** 778–86
[28] She G-L, Ren Y-R, Yuan F-G and Xiao W-S 2018 On vibrations of porous nanotubes *Int. J. Eng. Sci.* **125** 23–35
[29] She G-L, Yan K-M, Zhang Y-L, Liu H-B and Ren Y-R 2018 Wave propagation of functionally graded porous nanobeams based on non-local strain gradient theory *The European Physical Journal Plus* **133** 368
[30] Nejati M, Dimitri R, Tornabene F and Yas M H 2017 Thermal buckling of nanocomposite stiffened cylindrical shells reinforced by functionally graded wavy carbon nano-tubes with temperature-dependent properties *Applied Sciences* **7** 1–24
[31] Li X, Li L, Hu Y, Ding Z and Deng W 2017 Bending, buckling and vibration of axially functionally graded beams based on nonlocal strain gradient theory *Compos. Struct.* **165** 250–65
[32] Jouneghani F Z, Dimitri R and Tornabene F 2018 Structural response of porous FG nanobeams under hygro-thermo-mechanical loadings *Composites Part B: Engineering* **152** 71–8
[33] Malikan M and Dastjerdi S 2018 Analytical buckling of FG nanobeams on the basis of a new one variable first-order shear deformation beam theory *International Journal of Engineering & Applied Sciences* **10** 21–34
[34] Malikan M 2019 On the buckling response of axially pressurized nanotubes based on a novel nonlocal beam theory *Journal of Applied and Computational Mechanics* **5** 103–12
[35] Wang Y-Z, Wang Y-S and Ke L-L 2016 Nonlinear vibration of carbon nanotube embedded in viscous elastic matrix under parametric excitation by nonlocal continuum theory *Physica E: Low-Dimensional Systems and Nanostructures* **83** 195–200
[36] Benzair A, Tounsi A, Besseghier A, Heireche H, Moulay N and Boumia L 2008 The thermal effect on vibration of single-walled carbon nanotubes using nonlocal Timoshenko beam theory *J. Phys. D: Appl. Phys.* **41** 2254041
[37] She G-L, Yuan F-G, Karami B, Ren Y-R and Xiao W-S 2019 On nonlinear bending behavior of FG porous curved nanotubes *Int. J. Eng. Sci.* **135** 58–74
[38] Yazdani Sarvestani H and Ghayoor H 2016 Free vibration analysis of curved nanotube structures *Int. J. Non-Linear Mech.* **86** 167–73
[39] Fu Y M, Hong J W and Wang X Q 2006 Analysis of nonlinear vibration for embedded carbon nanotubes *J. Sound Vib.* **296** 746–56
[40] Jiang J, Wang L and Zhang Y 2017 Vibration of single-walled carbon nanotubes with elastic boundary conditions *Int. J. Mech. Sci.* **122** 156–66
[41] Song K, Zhang Y, Meng J, Green E C, Tajaddod N, Li H and Minus M L 2013 Structural polymer-based carbon nanotube composite fibers: understanding the processing–structure–performance relationship *Materials* **6** 2543–77
[42] Eringen A C 2002 *Nonlocal Continuum fIeld Theories* (New York: Springer)
[43] Mindlin R D and Eshel N N 1968 On first strain-gradient theories in linear elasticity *Int. J. Solids Struct.* **4** 109–24
[44] Sahmani S, Aghdam M M and Rabczuk T 2018 A unified nonlocal strain gradient plate model for nonlinear axial instability of functionally graded porous micro/nano-plates reinforced with graphene platelets *Mater. Res. Express* **5** 045048
[45] Malikan M and Nguyen V B 2018 Buckling analysis of piezo-magnetoelectric nanoplates in hygrothermal environment based on a novel one variable plate theory combining with higher-order nonlocal strain gradient theory *Physica E: Low-Dimensional Systems and Nanostructures* **102** 8–28
[46] Malikan M, Dimitri R and Tornabene F 2018 Effect of sinusoidal corrugated geometries on the vibrational response of viscoelastic nanoplates *Applied Sciences* **8** 1432
[47] Malikan M, Nguyen V B and Tornabene F 2018 Electromagnetic forced vibrations of composite nanoplates using nonlocal strain gradient theory *Mater. Res. Express* **5** 075031
[48] Malikan M, Dimitri R and Tornabene F 2018 Thermo-resonance analysis of an excited graphene sheet using a new approach *International Journal of Engineering & Applied Sciences* **10** 190–206
[49] Malikan M, Dimitri R and Tornabene F 2019 Transient response of oscillated carbon nanotubes with an internal and external damping *Composites Part B: Engineering* **158** 198–205
[50] Mehralian F and Beni Y T 2017 A nonlocal strain gradient shell model for free vibration analysis of functionally graded shear deformable nanotubes *International Journal of Engineering & Applied Sciences* **9** 88–102
[51] Zeighampour H, Tadi Beni Y and Karimipour I 2017 Material length scale and nonlocal effects on the wave propagation of composite laminated cylindrical micro/nanoshells *The European Physical Journal Plus* **132** 503
[52] Nematollahi M S, Mohammadi H and Ali Nematollahi M 2017 Thermal vibration analysis of nanoplates based on the higher-order nonlocal strain gradient theory by an analytical approach *Superlattices Microstruct.* **111** 944–59
[53] Nematollahi M S and Mohammadi H 2019 Geometrically nonlinear vibration analysis of sandwich nanoplates based on higher-order nonlocal strain gradient theory *Int. J. Mech. Sci.* **156** 31–45
[54] Mindlin R D 1965 Second gradient of strain and surface-tension in linear elasticity *Int. J. Solids Struct.* **1** 417–38
[55] Malikan M 2018 Buckling analysis of a micro composite plate with nano coating based on the modified couple stress theory *Journal of Applied and Computational Mechanics* **4** 1–15
[56] Malikan M 2017 Analytical predictions for the buckling of a nanoplate subjected to nonuniform compression based on the four-variable plate theory *Journal of Applied and Computational Mechanics* **3** 218–28
[57] Malikan M 2017 Electro-mechanical shear buckling of piezoelectric nanoplate using modified couple stress theory based on simplified first order shear deformation theory *Appl. Math. Modelling* **48** 196–207
[58] Malikan M 2018 Temperature influences on shear stability of a nanosize plate with piezoelectricity effect *Multidiscipline Modeling in Materials and Structures* **14** 125–42
[59] Malikan M 2018 Electro-thermal buckling of elastically supported double-layered piezoelectric nanoplates affected by an external electric voltage *Multidiscipline Modeling in Materials and Structures* **15** 50–78
[60] Malikan M and Sadraee Far M N 2018 Differential quadrature method for dynamic buckling of graphene sheet coupled by a viscoelastic medium using neperian frequency based on nonlocal elasticity theory *Journal of Applied and Computational Mechanics* **4** 147–60

[61] Malikan M, Jabbarzadeh M and Dastjerdi S 2017 Non-linear static stability of bi-layer carbon nanosheets resting on an elastic matrix under various types of in-plane shearing loads in thermo-elasticity using nonlocal continuum *Microsyst. Technol.* **23** 2973–91
[62] Golmakani M E, Malikan M, Sadraee Far M N and Majidi H R 2018 Bending and buckling formulation of graphene sheets based on nonlocal simple first order shear deformation theory *Mater. Res. Express* **5** 065010
[63] Malikan M, Tornabene F and Dimitri R 2018 Nonlocal three-dimensional theory of elasticity for buckling behavior of functionally graded porous nanoplates using volume integrals *Mater. Res. Express* **5** 095006
[64] Malikan M and Nguyen V B 2018 A novel one-variable first-order shear deformation theory for biaxial buckling of a size-dependent plate based on the Eringen's nonlocal differential law *World Journal of Engineering* **15** 633–45
[65] Li L, Hu Y and Ling L 2016 Wave propagation in viscoelastic single-walled carbon nanotubes with surface effect under magnetic field based on nonlocal strain gradient theory *Physica E: Low-dimensional Systems and Nanostructures* **75** 118–24
[66] Li L and Hu Y 2016 Wave propagation in fluid-conveying viscoelastic carbon nanotubes based on nonlocal strain gradient theory *Comput. Mater. Sci.* **112** 282–8
[67] Lim C W, Zhang G and Reddy J N 2015 A higher-order nonlocal elasticity and strain gradient theory and Its Applications in wave propagation *J. Mech. Phys. Solids* **78** 298–313
[68] Duan W-H, Wang C-M and Zhang Y-Y 2007 Calibration of nonlocal scaling effect parameter for free vibration of carbon nanotubes by molecular dynamics *J. Appl. Phys.* **101** 24305
[69] Ansari R, Sahmani S and Arash B 2010 Nonlocal plate model for free vibrations of single-layered graphene sheets *Physics Letters* A **375** 53–62
[70] Shaat M 2017 A general nonlocal theory and its approximations for slowly varying acoustic waves *Int. J. Mech. Sci.* **130** 52–63
[71] Lam D C C, Yang F, Chong A C M, Wang J and Tong P 2003 Experiments and theory in strain gradient elasticity *J. Mech. Phys. Solids* **51** 1477–508
[72] Li C, Lai S K and Yang X 2019 On the nano-structural dependence of nonlocal dynamics and its relationship to the upper limit of nonlocal scale parameter *Appl. Math. Modelling* **69** 127–41
[73] Gutierrez-Lemini D 2014 *Engineering Viscoelasticity* (Arlington, TX, USA: Springer) (https://doi.org/10.1007/978-1-4614-8139-3)
[74] Thai H-T 2012 A nonlocal beam theory for bending, buckling, and vibration of nanobeams *Int. J. Eng. Sci.* **52** 56–64
[75] Lu L, Guo X and Zhao J 2017 Size-dependent vibration analysis of nanobeams based on the nonlocal strain gradient theory *Int. J. Eng. Sci.* **116** 12–24
[76] Wang B, Deng Z, Ouyang H and Zhou J 2015 Wave propagation analysis in nonlinear curved single-walled carbon nanotubes based on nonlocal elasticity theory *Physica* E **66** 283–92